Available online at www.sciencedirect.com
SCIENCE DIRECT
Journal of Magnetic Resonance 180 (2006) 222–228
JMR Journal of Magnetic Resonance
www.elsevier.com/locate/jmr

# HACACO revisited: Residual dipolar coupling measurements and resonance assignments in proteins

Daniel O. Cicero [a], Gian Marco Contessa [a], Maurizio Paci [a], Renzo Bazzo [b,*]

[a] *Department of Chemical Science and Technology, University of Rome "Tor Vergata," Italy*
[b] *IRBM "P. Angeletti," Via Pontina km 30.600, 00040 Pomezia, Rome, Italy*

Received 1 December 2005; revised 24 January 2006
Available online 22 March 2006

**Abstract**

The revisited version of the HACACO experiment here presented, is more robust and straightforward to implement and continues to be, to a greater extent, a convenient tool for protein backbone resonance assignment. Additionally, it turns out to be a sensitive and accurate method to measure $C_\alpha$–$H_\alpha$ residual dipolar couplings (RDCs). The performance of our new pulse scheme for measurement of RDCs was tested on two proteins with different secondary structures: one characterized by a high β-sheet content, the second dominated by the presence of α-helices. In both examples the new method provided significantly more accurate data, compared to all previously published 3D techniques.


*Keywords:* HACACO; Residual dipolar couplings; Protein; Solution NMR

## 1. Introduction

Residual dipolar couplings (RDCs) are nowadays a valuable complement to NOEs in structure determination of proteins by NMR [1,2]. The range of application is largely determined by the capability of measuring a sufficient number of RDCs with sufficient accuracy, i.e., within an interval of confidence of only a few hertz, to generate valuable structural constraints. In general, resonance overlaps and signal line-widths typically would limit the application to proteins of small to medium size (MW up to 30 or 35 kDa). Isotope labeling allows a number of inter-nuclear vector orientations to be determined through RDC observation. Among them the amide N–H and $C_\alpha$–$H_\alpha$ RDCs are the most frequently used as structural restraints, mainly because they are the result of the largest dipolar interactions observable in a protein backbone, due to the large $^1$H gyromagnetic ratio and the short internuclear distances.

A first classification of the available methods for the measurement of $C_\alpha$–$H_\alpha$ coupling constants divides them into 2D and 3D experiments. Among the 2D methods we consider the $^{13}$C–$^1$H correlation, using constant-time HSQC [3] or $^{15}$N–$^1$H correlation using a (HACACO)NH experiment [4]. Although these methods in principle allow a high accuracy in the RDC measurement, often for most proteins two dimensions do not resolve many resonance overlaps. Hence the extension to 3D methods to improve resolution. They include experiments based on the HNCO [5], HN(CO)CA [6] , CB(CA)CONH [7], the (HA)CA(CO)NH [8] and its recent variation, the HA(CA)CONH [9].

In all such experiments the relevant parameters, determining the accuracy of the measurement of the observed coupling, are the signal-to-noise ratio (SN) and the linewidth (LW), in the dimension where the splitting is measured. Actually, a good estimate for the uncertainty in the measured splitting is the LW/SN ratio [6]. From this point of view, the HNCO or HN(CO)CA based experiments [5,6], although they seem to offer the best inherent sensitivity among all available experiments, since the

* Corresponding author. Fax: +39 06 91093 225.
*E-mail address:* renzo_bazzo@merck.com (R. Bazzo).

1090-7807/$ - see front matter © 2006 Elsevier Inc. All rights reserved.
doi:10.1016/j.jmr.2006.02.016

transverse magnetization resides on a slowly relaxing spin ($^{15}$N) during the long constant time periods, only offer a relatively limited resolution, since in practice the total evolution time in the $C_\alpha$ dimension cannot be conveniently extended beyond a time of about 10–12 ms. In fact, for longer evolution periods ($T$), the passive $C_\alpha$–$C_\beta$ coupling constant ($J = 35$ Hz) is simply reducing the signal by a factor $\cos(\pi JT)$. If this coupling remains unresolved, the resolution cannot be improved. The use of a 28 ms constant time period was proposed, to allow the detection of the $C_\alpha$–$H_\alpha$ coupling constant with improved resolution, since the $C_\alpha$–$C_\beta$ coupling is this time completely refocused. This is the basis of the (HA)CA(CO)NH experiment [8], which gives well-resolved signals, but, on the other hand, is less sensitive due to the use of long periods when transverse magnetization resides on $C_\alpha$ (fast relaxing), carbonyl (C′) and $^{15}$N nuclei. To reduce the sensitivity loss, a new scheme was recently proposed, in which the long constant time period on $C_\alpha$ is reduced from 28 to 7.6 ms and the $H_\alpha$–$C_\alpha$ coupling is monitored in a real-time manner exploiting the C′ dimension (Fig. 1) [9]. A significant improvement in sensitivity with respect to the (HA)CA(CO)NH is obtained. However, although the splitting to be measured now appears in the C′ dimension, via incorporation of the $H_\alpha$–$C_\alpha$ $J$ modulation into carbonyl evolution, the actual resolution of such splitting depends on the incrementation of the initial $H_\alpha$ period from zero to several ms (28 ms to achieve same resolution as in previous experiment). As a result the final peak LW depends on the proton $H_\alpha$ $T_2$ relaxation time, and also on all the unresolved $^1$H–$^1$H passive couplings, particularly RDC couplings, which can be many, for aligned molecules. For these reasons the peak LW in the end can still be quite unfavourable.

In the present work, we present an alternative experiment based on the HACACO [10] experiment that correlates $H_\alpha$, $C_\alpha$ and C′, a technique originally proposed for protein backbone assignment. We will show that a revisited version of the original HACACO experiment offers, on the one hand, a robust and useful tool to correlate inter-residue backbone resonances, and, on the other hand, a sensitive method for an accurate determination of $H_\alpha$–$C_\alpha$ RDCs. In fact in most cases the SN/LW ratio one can obtain turns out to be significantly better than with the previously described techniques.

## 2. Results and discussion

Let us first briefly revisit the HACACO experiment as it was originally proposed. Among the experiments designed to correlate intra-residue resonances, the pulse sequence HACACO [10] proved to be a valuable tool to obtain backbone chemical shift assignment of proteins (Fig. 2A). This experiment is indeed a natural extension of the 2D constant time proton-carbon correlation HSQC technique [11–13]. Simply one takes advantage of the long (~28 ms) $C_\alpha$ constant time evolution used in this experiment to monitor in the same interval the carbonyl spin evolution as well, with no need for additional evolution periods. In fact, coherence can easily be transferred to the carbonyl spins (under the form of $C_\alpha$–C′ multiple quantum coherence). After monitoring the C′ resonance frequencies in the typical available time of about 10–12 ms the coherence is again converted into Single Quantum coherence of $C_\alpha$ nuclei. The $C_\alpha$ frequencies are also monitored and then the magnetization is finally transferred to the $H_\alpha$ protons for detection.

In this work, we introduce a modified version ( Fig. 2B) of the original pulse sequence of the HACACO experiment [10] to take advantage of the complete 28 ms—long constant time for $C_\alpha$ frequency monitoring, with minimized phase distortions. This possibility already existed in the original version [10], although at the price of a more cumbersome implementation (see Fig. 2A legend for more details): namely, to maintain coherent $C_\alpha$–C′ coupling over the whole CT period, an additional C′ inversion pulse was needed to follow the $C_\alpha$ inversion pulse shifting outside the C′ central evolution time (dotted line in Fig. 2A). The point in this experiment is that the period in which carbonyl resonances evolve is nested inside the period in which also α-carbon resonances evolve . To simplify the execution of the pulse sequence we now introduce two $C_\alpha$ inversion pulses (Fig. 2B), symmetrically positioned in the constant time period at the beginning of the $C_\alpha$ evolution. Such

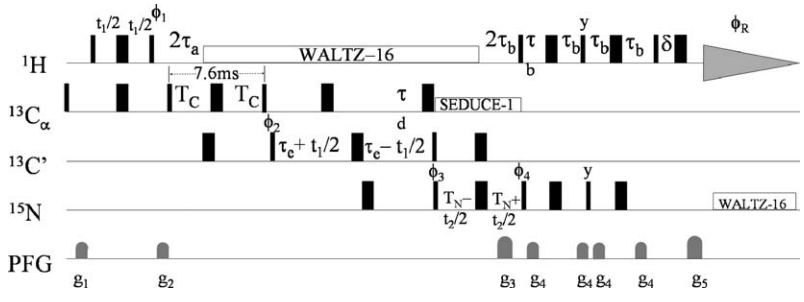


Fig. 1. Pulse scheme of the 3D HA(CA)CONH experiment [9] for measuring coupling constants of $C_\alpha$–$H_\alpha$. Narrow and wild bars represent 90° and 180° pulses. C′ represents carbonyl spin. All pulses are along $x$-axis unless indicated otherwise. Strengths and duration of gradients are: $g_1 = g_2 = (22.5$ G/cm, 0.5 ms), $g_3 = (33.75$ G/cm, 1.25 ms), $g_4 = (18$ G/cm, 0.5 ms), $g_5 = (32.56$ G/cm, 0.125 ms). The durations are $\tau_a = 1.8$ ms, $\tau_b = 2.35$ ms, $\tau_d = 4.5$ ms, $\tau_e = 14$ ms, $T_N = 14$ ms, $T_C = 3.8$ ms. Phase cycling is: $\phi_1 = y, -y$; $\phi_2 = y, y, -y, -y$; $\phi_3 = 4(x), 4(-x)$; $\phi_R = x, -x, -x, x, -x, x, x, -x$. Rance–Kay sensitivity enhancement scheme is used in $^{15}$N dimension.

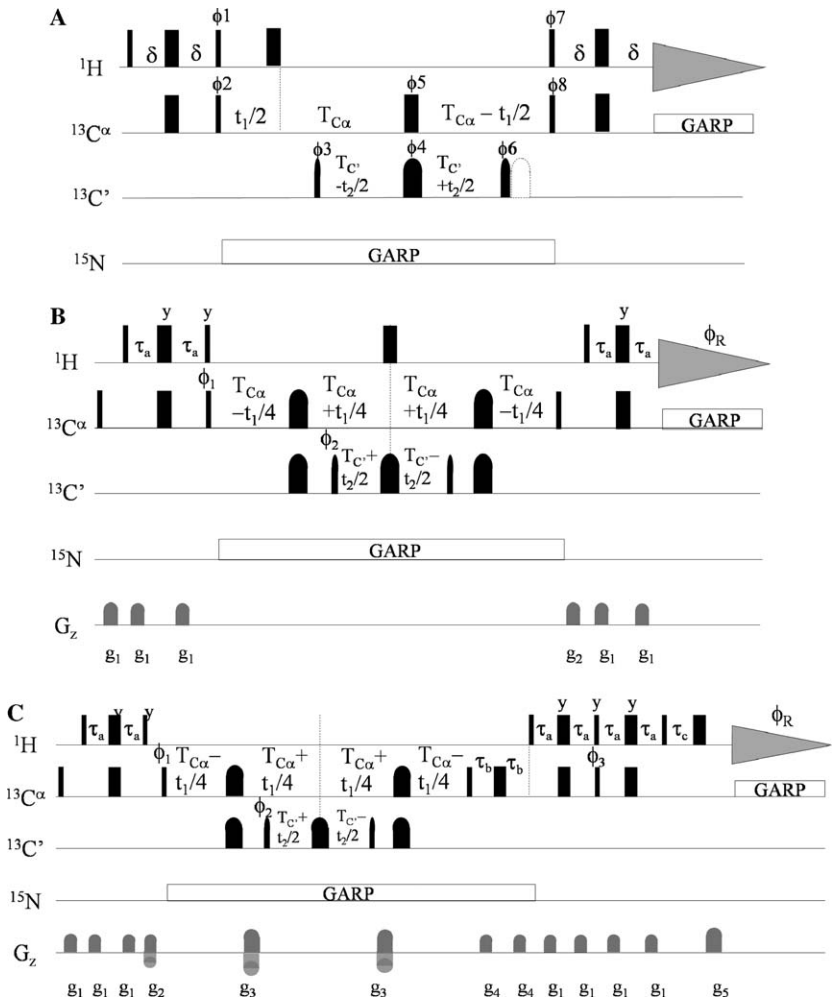


Fig. 2. Pulse schemes of the original 3D HACACO (A) [1] and revisited 3D HACACO (B and C) experiments for resonance assignment (A and B) and for measuring $C_\alpha$–$H_\alpha$coupling constants (C). Narrow and wide bars represent 90° and 180° pulses. C′ represents carbonyl spin. All pulses are along $x$-axis unless indicated otherwise. $^1$H and $^{15}$N carrier frequencies are at 4.7 and 119.8 ppm, respectively. $^{13}$C carrier frequency was kept at 55 ppm. For a proper C′ frequency sampling the ratio offset/SW must be an integer, where offset is the difference between $C_\alpha$ and C′ shaped pulse frequencies and SW is C′ spectral width. The power of decoupling GARP pulse is 1.25 kHz on $^{15}$N and 3.1 kHz on $^{13}$C. The $^{13}$C selective pulses are q5 for 90° and q3 for 180° and have a duration of 400 and 360 μs, respectively. (A) The durations are: $\delta = 1.6$ ms; $T_{C\alpha} = 14.56$ ms, $T_{CO} = 6$ ms. Phase cycling is: $\phi_1 = y$; $\phi_2 = x, -x$; $\phi_3 = x, x, -x, -x$; $\phi_4 = x, x, x, x, -x, -x, -x, -x$; $\phi_5 = x$; $\phi_6$ and $\phi_8$ are to be adjusted according to Bloch–Siegert effect; $\phi_7 = x$; $\phi_R = x, -x, -x, x$. The second 180° pulse on C′ (dotted line) is needed to maintain coherent (C′–$C_\alpha$) coupling if and when the 180° pulse on $C_\alpha$ is applied outside the C′ evolution time. Clearly, at that point the two inversion pulses have to be applied simultaneously (or, in practice, consecutively). This trick is necessary if one likes to exploit the complete $T_{C\alpha}$ period for monitoring $C_\alpha$ evolution and achieve best resolution. (B) The durations are $\tau_a = 1.6$ ms, $\tau_b = 0.5$ ms; $T_{C_\alpha} = 7.28$ ms, $T_{C'} = 6$ ms. Strengths and duration of gradients are: $g_1 = (5$ G/cm, 1 ms); $g_2 = (20$ G/cm, 0.5 m). All gradients are sine-shaped. Phase cycling is: $\phi_1 = x, -x$; $\phi_2 = x, x, -x, -x$; $\phi_R = x, -x, -x, x$. (C) The durations are $\tau_a = 1.6$ ms, $T_{C_\alpha} = 7.28$ ms, $T_{CO} = 6$ ms, $\tau_b$ = duration of $g_4$ and $\tau_c$ = duration of $g_5$. Strengths and duration of gradients are $g_1 = (2.5$ G/cm, 1 ms), $g_2 = (20$ G/cm, 2.5 ms), $g_3 = (42.8$ G/cm, 1.15 ms), $g_4 = (-6.5$ G/cm, 0.6 ms), $g_5 = (42.8$ G/cm, 578.46 μs). All gradients are sine-shaped. Quadrature detection for $C_\alpha$ was achieved inverting the $g_3$ polarity (and concomitantly $g_2$ polarity, to keep dephasing effect on water) and adding 180° to $\phi_3$, while quadrature detection for C′ was achieved adding 90° to $\phi_2$. Phase cycling is: $\phi_1 = x, x, -x, -x$; $\phi_2 = x, -x$; $\phi_3 = -y, -y, y, y$; $\phi_R = x, -x, -x, x$. Rance–Kay sensitivity enhancement scheme was used in $^1$H dimension.

pulses, are concertedly shifted in time backwards and forwards, respectively, to generate $C_\alpha$ spin evolution. Clearly, the two $C_\alpha$ inversion pulses are to be flanked by C′ inversion pulses as well, to maintain coherent $C_\alpha$–C′ coupling for the whole period. This simple trick allows the complete exploitation of the 28 ms—long constant time period for $C_\alpha$ frequencies monitoring, with optimized resolution and sensitivity. Moreover, such scheme prevents any phase distortion in the carbonyl signals since the complete carbonyl evolution is now not perturbed by extra $C_\alpha$ pulses. In the final pulse sequence, as reported in Fig. 2B, a proton inversion pulse is inserted at the center of the $C_\alpha$ evolution period to refocus the $C_\alpha$–$H_\alpha$ coupling.

Clearly, $^{13}C_\alpha$ transverse relaxation during the long constant time interval severely affects signal intensities, particularly for large molecules. In this respect it has been shown that to contrast carbon relaxation and increase sensitivity one could effectively use the slower decay of two-spin

coherence [14], since for methine groups the relaxation rate of $^{13}C$–$^{1}H$ two-spin coherence is slower than the relaxation rate of the individual $^{13}C$ and $^{1}H$ single spin coherences. Therefore, during the whole constant time period when the $C_\alpha$ coherence is evolving, the $H_\alpha$ coherence can also be maintained in the transverse plane, by omitting the second $^{1}H$ 90° pulse and applying a spin-lock field to $H_\alpha$ protons in order to "freeze" the $C_\alpha$–$H_\alpha$ two-spin coherence. Clearly, this scheme [14] is alternative to the use of the proton refocussing pulse in the middle of the sequence, as indicated in Fig. 2B. As recommended in the original paper [14], the spin lock field needs to be relatively low power (in practice less than about 1 kHz for a 600 MHz magnet) to prevent the spin locking of the relatively close (in frequency) magnetization components of β protons that would induce a proton–proton TOCSY-type transfer. For the same reason we observed that such a trick does not enhance sensitivity for glycine spin systems due to the unavoidable and undesired magnetization transfer between geminal protons. The same usually holds for serine and threonine residues since α and β protons can have quite close frequencies. For all other residues we observed a gain, usually between 30 and 40%. In summary, one has the choice between the two slightly different schemes, with the pros and cons just described: one with the $^{1}H$ refocusing pulse, as reported in Fig. 2B, and the other with the $^{1}H$ spin-lock field, as previously reported [14].

And here we finally come to a "natural" extra application of the present scheme: the measurement of $C_\alpha$–$H_\alpha$ residual dipolar couplings. Clearly, all the previously stated advantages also hold for this particular application. One has just to apply the sequence with no proton pulses during the constant time period of $C_\alpha$ evolution, which, as a result, will now incorporate the modulation due to the $C_\alpha$–$H_\alpha$ coupling. Extra $C_\alpha$–$H_i$ couplings, if at all present, are too small to affect sensitivity. The duration of the constant period (~28 ms) allows the high resolution that is necessary for the derivation of good quality structural constraints.

The pulse sequence for residual dipolar coupling measurements is reported in Fig. 2C. A more elaborated gradient scheme here makes this experiment perfectly feasible for water ($H_2O$) samples, hence practical for samples of proteins in partially oriented media. The latter is not a trivial point, since, although the HACACO experiment per se can obviously be conveniently performed in $D_2O$, one usually needs to measure several types of RDCs, like for

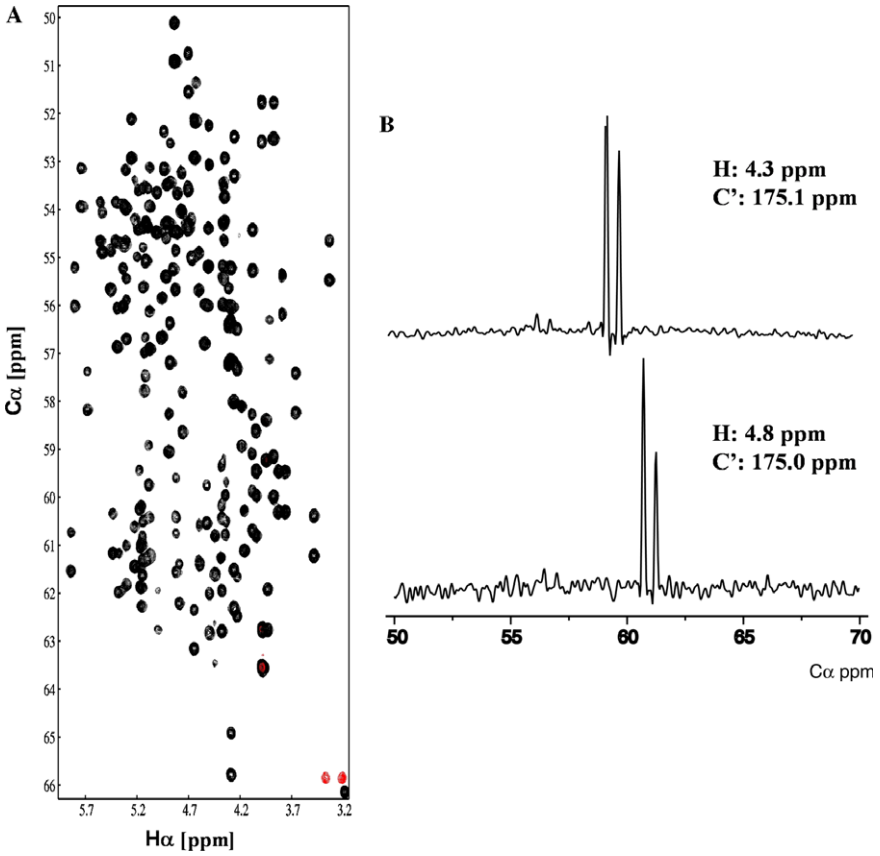


Fig. 3. Selected spectra to show the "effective" elimination of water signal. (A) Projection of all the $H_\alpha$–$C_\alpha$ planes of the HACACO experiment performed with the pulse sequence of Fig. 2C on the ApaG protein 0.5 mM in 95% $H_2O$, 5% $D_2O$ (see additional experimental details in Fig. 4). C′ represents carbonyl spin. (B) Traces of two $H_\alpha$–$C_\alpha$ peak doublets, at $^{1}H$ 4.3 ppm and $^{13}C'$ 175.1 ppm for the upper trace and at $^{1}H$ 4.78 ppm and $^{13}C'$ 175.0 ppm for the lower trace. The $^{1}H$ shift in the lower trace precisely coincides with the chemical shift of water. By comparison between the two traces, a barely observable little extra noise is all that is left of the strong water signal.

instance NH RDCs, on the same sample, to guarantee that such measurements refer to the same alignment conditions. Hence the practical need to be able to measure $C_\alpha$ RDCs in $H_2O$. The rationale for water suppression via the gradient scheme illustrated in Fig. 2C is summarized as follows. Immediately following the second 90° proton pulse the water magnetization lies in the transverse plane and needs to be dephased by a sufficient strong gradient ($g_2$), to avoid radiation damping to restore most of its intensity along the $z$-axis. Later in the pulse sequence two more strong gradients ($g_3$) are used both for encoding α carbon phase and to further destroy any residual transverse water magnetization. At the end of the constant time period, water magnetization will have retrieved only a very small net component along the $z$-axis, via proper $T_1$ relaxation. We empirically found that an additional couple of short gradients ($g_4$) may be used at this point to ensure that absolutely no transverse components remain. The small ($T_1$ restored) positive $z$-component is then coherently taken through the different steps of the sensitivity enhancement block until it

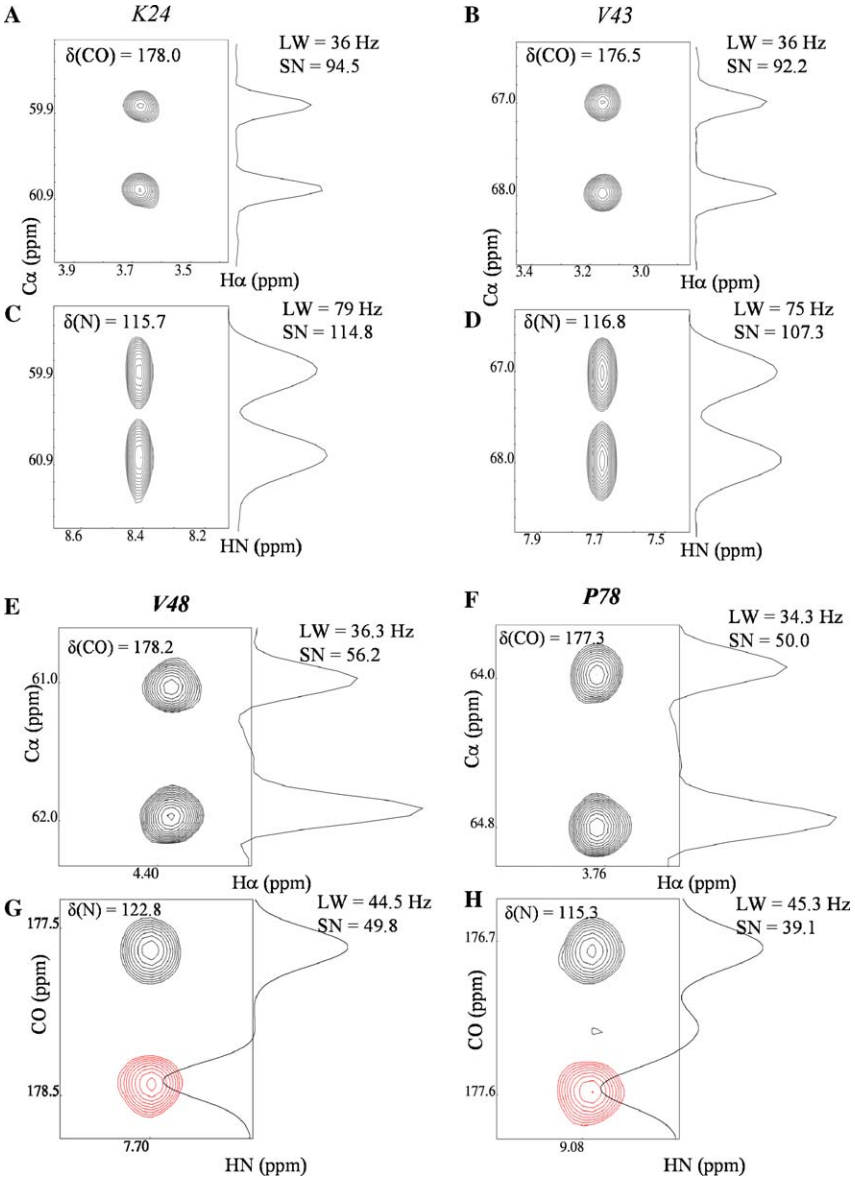


Fig. 4. Selected slices of spectra acquired using revisited HACACO (A and B), HN(CO)CA (C and D) experiments on Myosin Light Chain Mlc1p and revisited HACACO (E and F), HA(CA)CONH (G and H) on the ApaG protein. C′ represents carbonyl spin. The slices were extracted at C′ = 178.0, 176.5, 178.2 and 177.3 ppm (A, B, E, F, respectively) and $^{15}N = 115.7$, 116.8, 122.8 and 115.3 ppm (C, D, G, H, respectively). The concentration of the sample of ApaG was 0.5 using 40 mM $NaH_2PO_4$ (pH 6.8), 50 mM NaCl, 0.05% NaN3 (95% $H_2O$ and 5% $D_2O$) while the concentration of Mlc1p was 0.8 in 50 mM phosphate buffer (pH 6.8) and 0.3 M NaCl. NMR spectra were collected at 298 °C on a 600 MHz Bruker Avance spectrometer with cryprobe for Mlc1p and at 303 °C on a 700 MHz Bruker Avance spectrometer for ApaG, with 16 scans per FID. The total experimental times are 93 h for all the experiments. Both $t_1$ and $t_2$ time domains were apodized using a sine-bell window function with exponent two. The digital resolution in $F_1$ was improved by zero-filling the $t_1$ time domain to 128 prior to Fourier transformation. The data points of $t_2$ time domain were zero-filled to 512 prior to transformation. The $t_3$ domain was apodized using a Gaussian window function and the data was zero-filled to 1024 points prior to transformation.

Table 1
Average linewidth (LW), signal-to-noise ratio (SN) and $\Delta J$ obtained with the HN(CO)CA, HACACO, and HA(CA)CONH experiments acquired on the MLC1p and ApaG proteins

| | Experiment | LW (Hz) | SN | $\Delta J = LW/SN$ (Hz) |
|---|---|---|---|---|
| Mlc1p | HN(CO)CA | $81.7 \pm 9.4$ | $72.8 \pm 30.3$ | 1.4 |
| | HACACO | $35.4 \pm 1.8$ | $81.7 \pm 27.1$ | 0.5 |
| ApaG | HA(CA)CONH | $46.0 \pm 3.3$ | $11.9 \pm 13.2$ | 3.9 |
| | HACACO | $35.6 \pm 2.1$ | $20.8 \pm 14.1$ | 1.7 |

is finally put back along the original $+z$ direction. Any residual transverse component that might still be present at the end, due to pulse imperfections (or whatever reason), is completely annihilated by the quite strong gradient $g_5$, the last signal refocusing gradient, just before detection. Empirically, we did not find it more convenient to use a couple of gradients with half strength and opposite signs at the two sides of the last proton inversion pulse, to reduce eddy currents. As a result of this careful choice of gradient pulses, the detected signal is at the end completely deprived of any contribution from water magnetization, as one can see in Fig. 3 where $C_\alpha$–$H_\alpha$ peaks are shown exactly at the water resonance position.

A final significant element to evaluate the HACACO experiment, in which two dimensions are $H_\alpha$–$C'$, in comparison with other methods in which for example two dimensions are NH–N, is the percentage of resolved signals that can be ultimately detected. As it is well known that the NH–N dimensions offer better resonance dispersion than the $H_\alpha$–$C'$ dimensions and that such difference strongly depends on the protein secondary structure as well, the performance of our new pulse scheme was tested on two different proteins: the ApaG protein from *Xanthomonas axonopodis* pv. *citri* [15] and the calmodulin-like myosin light chain 1 (Mlc1p) from *Saccharomyces cerevisiae* [16]. The ApaG protein (127 residues) has a secondary structure with high β-sheet content, while MLC1p (149 residues) has a secondary structure dominated by the presence of α-helices. Experimental conditions and data processing are discussed in the caption of Fig. 4, where selected examples are shown.

To compare the efficacy of the new pulse sequence with other ones previously mentioned, the HN(CO)CA and HACACO spectra were acquired on Mlc1p, while the HA(CA)CONH and HACACO spectra were acquired on the ApaG protein, using identical experimental conditions. For the ApaG protein, the resonance dispersion allowed by the $C'$ nucleus enables to measure RDCs for 88% of the residues, with a significantly higher accuracy with respect to the HN(CO)CA sequence (see Table 1). This result is due to the longer evolution time used in the $C_\alpha$ dimension (28 ms for the HACACO vs 10–12 ms for the HN(CO)CA), while the SN ratio is similar in the two spectra. For Mlc1p, with a predominantly α-helical secondary structure, the $C'$ dimension has a lower dispersion, however sufficient to allow accurate measurements of the $H_\alpha$–$C_\alpha$ RDCs (see Table 1) for 75% of the amino-acids. Even in the case of Mlc1p, the LW/SN ratio of the HACACO spectrum is better than for the competing HA(CA)CONH sequence, because the peak LW in the HA(CA)CONH spectrum is negatively determined by the evolution of the $H_\alpha$ nucleus, as previously explained, while the compact scheme of the HACACO ensures a predetermined resolution (the same for all peaks, fixed by the length of the constant time of 28 ms) and an overall better sensitivity.

In summary, we have shown that a revisited form of the HACACO experiment, while on the one hand is still a valuable tool for protein backbone assignment, on the other hand turns out to be an extremely convenient technique for measuring $H_\alpha$–$C_\alpha$ RDCs with optimized resolution and sensitivity.

## Acknowledgments

We are grateful to Matteo Pennestri, Sonia Melino, Thelma Pertinhez, Alberto Spisni, Chuck Farah, and Antonella Ragnini for kindly providing the protein samples, and to Fabio Bertocchi for technical support. This work was partially supported by MIUR PRIN projects and the MIUR FIRB fundings.

## References

[1] J.R. Tolman, J.M. Flanagan, M.A. Kennedy, J.H. Prestegard, Nuclear Magnetic Dipole Interactions in Field-Oriented Proteins: Information for Structure Determination in Solution, Proc. Natl. Acad. Sci. USA 92 (1995) 9279–9283.
[2] N. Tjandra, A. Bax, Direct measurement of distances and angles in biomolecules by NMR in a dilute liquid crystalline medium, Science 278 (1997) 1111–1114.
[3] N. Tjandra, A. Bax, Measurement of dipolar contributions to $^1$JCH splittings from magnetic field dependence of $J$ modulation in two-dimensional NMR spectra, J. Magn. Reson. 124 (1997) 512–515.
[4] T.K. Hitchens, S.A. McCallum, G.S. Rule, A $J^{CH}$-Modulated 2D (HACACO)NH Pulse Scheme for Quantitative Measurement of $^{13}C^\alpha$–$^1H^\alpha$ Couplings in $^{15}N$, $^{13}C$-Labeled Proteins, J. Magn. Reson. 140 (1999) 281–284.
[5] D. Yang, J. Tolman, N.K. Goto, L.E. Kay, An HNCO-based Pulse Scheme for the Measurement of 13Cα-1Hα One-bond Dipolar couplings in 15N, 13C Labeled Proteins, J. Biomol. NMR 12 (1998) 325–332.
[6] A. Bax, G. Kontaxis, N. Tjandra, Dipolar couplings in macromolecular structure determination, Methods Enzymol. 339 (2001) 127–174.
[7] J.J. Chou, A. Bax, Protein sidechain rotamers from dipolar couplings in a liquid crystalline phase, J. Am. Chem. Soc. 123 (2001) 3844–3845.
[8] N. Tjandra, A. Bax, Large variations in $^{13}C_\alpha$ chemical shift anisotropy in proteins correlate with secondary structure, J. Am. Chem. Soc. 119 (1997) 9576–9577.
[9] W. Hu, Z. Zhang, Y. Chen, A high sensitivity 3D experiment for measuring $C_\alpha$–$H_\alpha$ residual dipolar coupling constants, J. Magn. Reson. 165 (2003) 248–252.

[10] R. Bazzo, D.O. Cicero, G. Barbato, A New 3D HCACO Pulse Sequence with Optimized Resolution and Sensitivity. Application to the 21 kDa Protein Human Interleukin-6, J. Magn. Reson. Ser. B 107 (1995) 189–191.

[11] J. Santoro, G.C. King, A Constant-Time 2D Overbodenhausen Experiment for Inverse Correlation of Isotopically Enriched Species, J. Magn. Reson. 97 (1992) 202–207.

[12] F.J.M. van de Ven, M.E.P. Philippens, Optimization of Constant-Time Evolution in Multidimensional NMR Experiments, J. Magn. Reson. 97 (1992) 637–644.

[13] G.W. Vuister, A. Bax, Resolution Enhancement and Spectral Editing of Uniformly 13CEnriched Proteins by Homonuclear Broadband 13C Decoupling, J. Magn. Reson. 98 (1992) 428–435.

[14] S. Grzesiek, A. Bax, Spin-locked multiple quantum coherence for signal enhancement in heteronuclear multi-dimensional NMR experiment, J. Biomol. NMR 6 (1996) 335–339.

[15] Â.M. Katsuyama, D.O. Cicero, A. Spisni, M. Paci, C.S. Farah, T.A. Pertinhez, Letter to the Editor: $^{1}H$, $^{15}N$ and $^{13}C$ Resonance Assignments of the ApaG Protein of the Phytopathogen *Xanthomonas Axonopodis* pv. *citri*, J. Biomol. NMR 29 (2004) 423–424.

[16] S. Melino, M. Pennestri, A. Santoprete, P. Bielli, M. Paci, A. Ragnini-Wilson, D.O. Cicero, Letter to the Editor: Assignment of the $^{1}H$, $^{13}C$ and $^{15}N$ resonances of Mlc1p from *Saccharomices cerevisiae*, J. Biomol. NMR 31 (2005) 367–368.